Electron-electron interaction effects in transport through open dots: Pinning of resonant levels

S. Ihnatsenka and I. V. Zozoulenko
Solid State Electronics, Department of Science and Technology (ITN), Linköping University, 60174 Norrköping, Sweden

M. Willander
Solid State Electronics, Department of Science and Technology (ITN), Linköping University, 60174 Norrköping, Sweden
and Department of Physics, Göteborg University, 412 96 Göteborg, Sweden

(Received 5 January 2007; revised manuscript received 29 March 2007; published 6 June 2007)

The role of electron-electron interaction in transport properties of open quantum dots is studied. The self-consistent full quantum-mechanical magnetotransport calculations within the Hartree, density-functional theory, and Thomas-Fermi approximations were performed, where a whole device, including the semi-infinitive leads, is treated on the same footing (i.e., the electron-electron interaction is accounted for both in the leads as well as in the dot region). The main finding of the present paper is the effect of pinning of the resonant levels to the Fermi energy due to the enhanced screening. Our results represent a significant departure from a conventional picture where a variation of external parameters (such as a gate voltage, magnetic field, etc.) causes the successive dot states to sweep past the Fermi level in a linear fashion. We instead demonstrate the highly nonlinear behavior of the resonant levels in the vicinity of the Fermi energy. The pinning of the resonant levels in open quantum dots leads to the broadening of the conduction oscillations in comparison to the one-electron picture. The effect of pinning becomes much more pronounced in the presence of the perpendicular magnetic field. This can be attributed to the enhanced screening efficiency because of the increased localization of the wave function. The strong pinning of the resonant energy levels in the presence of magnetic field can have a profound effect on transport properties of various devices operating in the edge state transport regime. We also critically examine an approximation often used in transport calculations where an inherently open system is replaced by a corresponding closed one.

DOI: 10.1103/PhysRevB.75.235307 PACS number(s): 73.23.Ad, 73.63.Nm, 73.21.La, 72.15.Gd

I. INTRODUCTION

A transport regime where a submicron lateral structure is strongly coupled to electron reservoirs (leads) is usually referred to as an open one.[1,2] This transport regime can be realized in quantum wires, dot, and antidot structures typically fabricated using a split gate or related techniques. Such techniques allow one to obtain devices with desired and variable geometry and parameters such as electron density and lead openings. The quantum dot operates in an open regime when the gate voltage sets up two quantum point contacts (QPCs) at the entrance and exit of the dot such that they transmit one or more channels (i.e., the conductance of an individual QPC, $G_{QPC} \gtrsim \frac{2e^2}{h}$). In this regime, electrons can freely enter and exit the dot, such that the electron number inside the dot is not integer and the chemical potential throughout the whole device in the linear-response regime is constant. (Opposite regime emerges when the point contacts are nearly pinched off and is referred to as a Coulomb blockade.[2,3] In this case, the electron number in the dot is quantized and the chemical potential inside the dot is different from that in the leads.) During the past decade, the open quantum dots have received a significant attention, providing many important insights into areas such as quantum interference, chaos, decoherence, localization, and many others.[1] Earlier transport experiments have been mainly devoted to the dots with hundreds or even thousands of electrons. Only recently it has become possible to reduce occupancy down to only a few or even one electron.[4,5]

Electron-electron interaction is known to have a great impact on transport in quantum dots with such pronounced examples as Coulomb blockade[3] or Kondo effect.[6] A description of the quantum transport in quantum dots is often based on model Hamiltonians containing phenomenological parameters such as coupling strengths or charging constants.[7–9] In many cases it is not always straightforward to relate quantitatively the above parameters to the physical processes they represent in the real system and sometimes it is not even obvious whether a model description is sufficient to capture the essential physics. At the same time, it is now well recognized that a detailed understanding and interpretation of the experiment might require a quantitative microscopical modeling of the system at hand, free from phenomenological parameters and not relying on model Hamiltonians which validity is poorly controlled. The importance of such modeling can be illustrated by examples including the quantitative description of the compressible and/or incompressible strips in magnetic field at the edges of the two-dimensional electron gas[10] or explanation of the Hund rule observed in few-electron quantum dots,[11] just to name a few.

The purpose of the present paper is twofold. First, we develop an approach aimed on full quantum-mechanical many-body transport calculations in open systems that starts from the lithographical layout of the device and does not include phenomenological parameters such as coupling strengths, charging constants, etc. The whole device, including semi-infinitive leads, is treated on the same footing (i.e., the electron-electron interaction is accounted for both in the leads and in the dot region). Using the recursive Green's-function technique, we self-consistently compute the scattering solutions of the two-dimensional Schrödinger equation in magnetic field.[12] Following the parametrization for the ex-

change and correlation energy functionals of Tanatar and Ceperley,[13] the electron-electron interaction is incorporated within the density-functional theory (DFT) in the local-density approximation.[11,14] The validity of the DFT approximation is supported by the excellent agreement with the exact diagonalization and variational Monte Carlo calculations performed for few-electron systems[15] as well as by the good quantitative correspondence between the experiment and the DFT calculations for the magnetoconductance of quantum wires.[16] Our approach thus accounts for the quantum mechanics nature of the scattering states and the resonant levels as well as for the exchange and correlation beyond the Hartree approximation. At the same time, it accurately describes the global electrostatic and the screening in the dots as well as in the leads.

The second aim of the present paper is to revise the role of the electron-electron interaction in transport properties of open quantum dots. It is widely believed that in open transport regime (as opposed to the Coulomb blockade or Kondo regime), the electron-electron interaction plays only a minor role. The main finding of the present paper is the effect of pinning of the resonant levels to the Fermi energy due to the enhanced screening. Our results represent a significant departure from a conventional picture adopted in most model Hamiltonians as well as in more sophisticated numerical calculations where a variation of external parameters (such as a gate voltage, magnetic field, etc.) causes the successive dot states to sweep past the Fermi level in a linear fashion. We instead demonstrate the highly nonlinear behavior of the resonant levels in the vicinity of the Fermi energy. One of the observable consequence of this effect is the smearing of the conductance fluctuations. We also show that the resonant level pinning becomes especially pronounced in magnetic field. Thus, accounting for this effect might be important for the interpretation of the magnetotransport experiment in open structures, including, e.g., recent studies of the electronic Mach-Zehnder interferometer[17] and the Laughlin quasiparticle interferometer,[18] structures designed to test the realization of the topological quantum computing,[19] antidot structures,[20–22] and others. It should also be noted that the quantum dot structures demonstrating Kondo effect fall into the semiopen transport regime such that accounting for the effect of the nonlinear screening leading to the resonant level pinning might be essential for the interpretation of the experiments in this regime as well.

Finally, a comment is in order concerning the applicability of the developed method. The conductance calculations in open quantum dots presented in this paper are based on an approach (often referred to as NGFT+DFT) that during recent years became a standard tool for transport *ab initio* calculations in molecular junctions, atomic wires, and related systems.[23–31] Its starting point is the Landauer-type formula, where the conductance is calculated using the nonequilibrium Green's-function technique (NGFT) or similar methods combined with the density-functional theory in the local-density approximation. This approach witnessed a great success in reproducing observed *I-V* characteristics of molecular and metallic junctions, notably in the strong coupling limit (when the conductance exceeds the conductance unit $G_0 = 2e^2/h$). At the same time, for weakly coupled systems such as organic molecules, the standard NGFT+DFT approach leads to the orders-of-magnitude discrepancy between the measured and calculated currents and to incorrect predictions of the conducting (instead of experimentally observed insulated) phase.[26–30] It has been recently recognized that the failure of this approach in the weak-coupling regime can be traced to spurious self-interaction errors caused by the lack of the derivative discontinuity of the exchange and correlation potentials in the standard DFT.[26–31] It has been demonstrated recently that elimination of the self-interaction errors and restoring agreement with the experiment for the case of the weak coupling require approaches and the exchange and correlation functionals that go beyond the standard NGFT+DFT scheme.[26–30] Because of this, our present mean-field approach is not expected to work for the case of the weak coupling (i.e., when the conductance of each QPC connecting the dot to the reservoir is reduced below the conductance unit G_0), and its applicability is limited to the open dot regime when the electron number in the dot is not quantized and the Coulomb charging is unimportant.

The paper is organized as follows. Section II presents the model and the Hamiltonian of the system at hand. In Sec. III, the numerical method for the self-consistent calculation of the magnetoconductance is described. Computational results are presented and discussed in Sec. IV, and conclusions are given in Sec. V.

II. MODEL

We consider an open quantum dot attached to semi-infinitive leads (electron reservoirs) in a perpendicular magnetic field B. A schematic layout of the device is illustrated in Fig. 1(a). Charge carriers originating from a fully ionized donor layer form the two-dimensional electron gas (2DEG), which is buried inside a substrate at the GaAs/$Al_xGa_{1-x}As$ heterointerface situated at a distance b from the surface. Metallic gates placed on the top of the heterostructure define the dot and the leads on the depth of the 2DEG [Figs. 1(a) and 1(b)].

The Hamiltonian of the whole system (the dot+the leads) can be written in the form

$$H = H_0 + V(\mathbf{r}), \tag{1}$$

where H_0 is the kinetic energy in the Landau gauge, $\mathbf{A}=(-By,0,0)$,

$$H_0 = -\frac{\hbar^2}{2m^*}\left\{\left(\frac{\partial}{\partial x} - \frac{eiBy}{\hbar}\right)^2 + \frac{\partial^2}{\partial y^2}\right\}, \tag{2}$$

$\mathbf{r}=(x,y)$, and $m^*=0.067m_e$ is the GaAs effective mass. The total confining potential within the framework of the density-functional theory is the sum of the electrostatic confinement potential, the Hartree potential, and the exchange-correlation potential

$$V(\mathbf{r}) = V_{conf}(\mathbf{r}) + V_H(\mathbf{r}) + V_{xc}(\mathbf{r}). \tag{3}$$

The electrostatic confinement $V_{conf}(\mathbf{r})=V_{gates}(\mathbf{r})+V_{donors}+V_{Schottky}$ includes contributions, respectively, from the top gates, the donor layer, and the Schottky barrier. The explicit

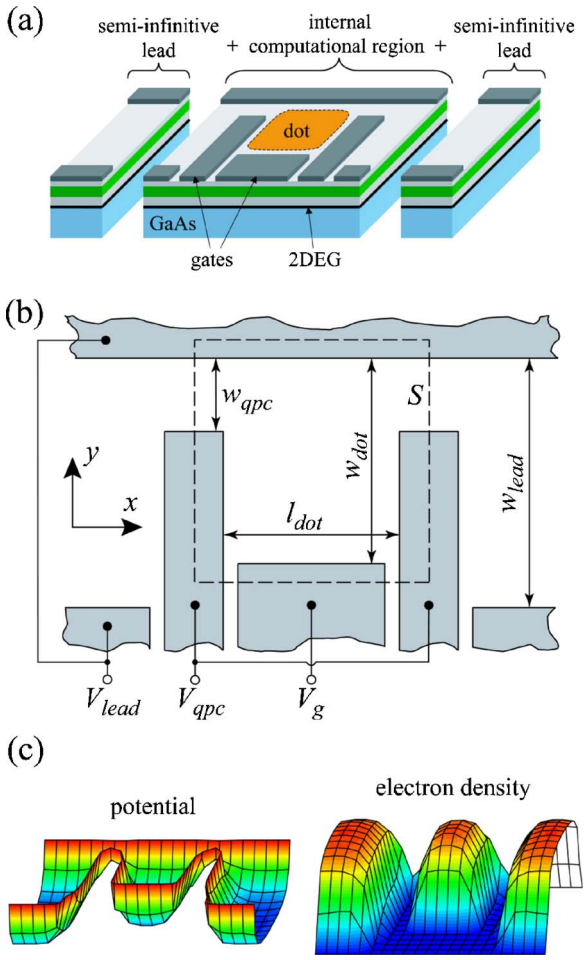

FIG. 1. (Color online) (a) Structure of an open quantum dot. The internal region is attached to two semi-infinitive quantum wires which serve as the electron reservoirs. (b) The layout of the gates defining the dot. The dashed line defines the area S of the quantum dot used to calculate a number of electrons in it. (c) Representative calculated self-consistent potential and the electron density.

expressions for the potentials $V_{gates}(\mathbf{r})$ and V_{donors} are given respectively in Refs. 32 and 33; the Schottky barrier is chosen to be $V_{Schottky}=0.8$ eV. The Hartree potential is written in a standard form

$$V_H(\mathbf{r}) = \frac{e^2}{4\pi\varepsilon_0\varepsilon_r}\int d\mathbf{r}' n(\mathbf{r}')\left(\frac{1}{|\mathbf{r}-\mathbf{r}'|} - \frac{1}{\sqrt{|\mathbf{r}-\mathbf{r}'|^2+4b^2}}\right), \tag{4}$$

where $n(\mathbf{r})$ is the electron density, the second term describes the mirror charges placed at a distance b from the surface, $n(\mathbf{r})$ is the electron density, $\varepsilon_r=12.9$ is the dielectric constant of GaAs, and the integration is performed over the whole device area including the semi-infinite leads.

The last term in the total confining potential (3) is the exchange and correlation potentials $V_{xc}[n(\mathbf{r})]=V_x[n(\mathbf{r})]+V_c[n(\mathbf{r})]$, which is the functional of the electron density. In the local-density approximation, it is given by a functional derivative[14]

$$V_{xc} = \frac{d}{dn}\{n\epsilon_{xc}(n)\}. \tag{5}$$

For ϵ_{xc} we have used the parametrization of Tanatar and Ceperley[13] for the case of spin-degenerate electrons. In particular, for the exchange potential this parametrization gives $V_x[n(\mathbf{r})]=-\frac{e^2}{\varepsilon_0\varepsilon_r\pi^{3/2}}\sqrt{n(\mathbf{r})/2}$. Note that by setting $V_{xc}(\mathbf{r})=0$ in Eq. (3), we reduce our approach to the standard Hartree approximation.

To outline the role of quantum-mechanical effects in the electron-electron interaction in open quantum dots, we also consider the Thomas-Fermi (TF) approximation. In this approximation, the kinetic energy is related to the electron density,[14] $H_0=\frac{\pi\hbar^2}{m^*}n(\mathbf{r})$. The self-consistent electron density is, thus, obtained from the solution of the equation

$$\frac{\pi\hbar^2}{m^*}n(x,y) + V_{conf}(r) + V_H(r) = E_F. \tag{6}$$

The electron density and the total confining potential calculated within the TF approximation do not capture quantum-mechanical quantization of the electron motion. The utilization of the TF approximation for the modeling of the magnetotransport in an open system is, therefore, conceptually equivalent to a one-electron approach. The difference between these approaches is the shape of the total confining potential: in one-electron transport simulations, one typically starts with a model hard-wall confinement, whereas the TF approximation gives a rather smooth potential which represents a good approximation to the actual confinement.

III. METHOD

The magnetoconductance through the quantum dot in the linear-response regime is given by the Landauer formula[34]

$$G = -\frac{2e^2}{h}\int dE T(E)\frac{\partial f_{FD}(E-E_F)}{\partial E}, \tag{7}$$

where $T(E)$ is the total transmission coefficient, $f_{FD}(E-E_F)$ is the Fermi-Dirac distribution function, and E_F is the Fermi energy. In order to calculate $T(E)$ in perpendicular magnetic field, we utilize the recursive Green's-function technique in the hybrid energy-space representation.[12] We discretize Eq. (1) and introduce the tight-binding Hamiltonian (with lattice constant $a=4$ nm), where the perpendicular magnetic field is included in a form of Peierl's substitution.[34] The retarded Green's function is introduced in a standard way,[34]

$$\mathcal{G} = (E - H + i\eta)^{-1}. \tag{8}$$

The Green's function in the real-space representation, $\mathcal{G}(\mathbf{r},\mathbf{r},E)$, provides an information about the electron density at the site $\mathbf{r}$,[34]

$$n(\mathbf{r}) = -\frac{1}{\pi}\Im\int dE\mathcal{G}(\mathbf{r},\mathbf{r},E)f(E-E_F). \tag{9}$$

Note that $\mathcal{G}(\mathbf{r},\mathbf{r},E)$ is a rapidly varying function of energy. As a result, a direct integration along the real axis in Eq. (9) is rather ineffective as its numerical accuracy is not sufficient

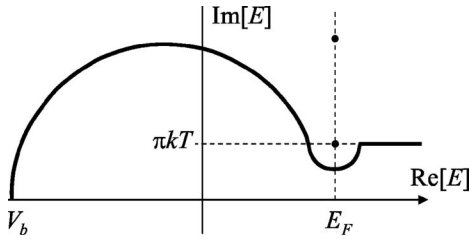

FIG. 2. A typical integration contour used in the calculation of integral (9). Dots indicate the poles of the Fermi-Dirac distribution function in the upper complex plane at $\Re[E]=E_F$, $\Im[E]=(2m+1)\pi kT$, $m=0,1,2,\ldots$. V_b is the bottom of the conduction band in the leads (the lowest potential in the system).

to achieve convergence of the self-consistent electron density. Because of this, we transform the integration contour into the complex plane $\Im[E]>0$, where the Green's function is much more smoother. Note that all poles of the retarded Green's function are in the lower half plane $\Im[E]<0$. A typical contour used in the integration, avoiding poles of the Fermi-Dirac function, is shown in Fig. 2.

In order to calculate the Green's function of the whole system dot+leads, we divide the system into three parts, the internal computational region and two semi-infinite leads, as shown in Fig. 1(a). Note that the internal region incorporates not only the dot but also the straight segments, including a part of the leads. We place the semi-infinite leads sufficiently far away from the dot where the total self-consistent potential and the electron density do not change along the leads (i.e., the electron density and the potential in the leads are not affected by the internal region such that the leads can be considered as uniform quantum wires). This allows us to calculate the total potential and the electron density in the lead regions using the technique developed in Ref. 35 for an infinite homogeneous channel in the perpendicular magnetic field. The Green's function in the internal region is calculated using the standard recursive Green's-function technique. The total Green's function for the whole system is calculated by linking, with the help of the Dyson equation, the surface Green's function for the semi-infinite leads (with the self-consistent potential calculated using the technique in Ref. 35) and the Green's function of the internal region.

All the calculations described above are performed self-consistently in an iterative way until a converged solution for the electron density and potential (and hence for the total Green's function) is obtained. Having calculated the total self-consistent Green's function, the scattering problem is solved where the scattering states in the leads (both propagating and evanescent) are obtained using the Green's-function technique of Ref. 35. (The equation for the calculation of the transmission and reflection coefficients using the Green's function in the presence of the magnetic field is derived in Ref. 12.)

Having calculated the Green's function of the internal region and the wave function in the leads, we can recover the wave function $\psi(\mathbf{r},E)$ inside the internal region. For visualization of the wave function inside the dot, we include the effect of the finite temperature as follows:

$$|\Psi(\mathbf{r})|^2 = -\int dE|\psi(\mathbf{r},E)|^2\frac{\partial f_{FD}(E-E_F)}{\partial E}. \tag{10}$$

In order to find the density of states (DOS) inside the quantum dot,[34] we perform integration over the dot area S defined in Fig. 1(b),

$$\mathrm{DOS}(E) = -\frac{1}{\pi}\Im\int_S d\mathbf{r}\mathcal{G}(\mathbf{r},\mathbf{r},E). \tag{11}$$

Note that a many-body approach, conceptually similar to ours, for calculation of the quantum transport in an open dot was developed in Ref. 36 for the case of zero magnetic field. The magnetic field was included in the dot region in the transport calculations presented in Ref. 37, where, however, the leads were considered as noninteracting.

As we mentioned in the previous section, we also employ the TF approximation for the calculation of the magnetotransport through the quantum dot. This calculation is done by the same method as described above, with the only difference that the self-consistent electron densities in the internal region and in the semi-infinite leads are calculated from the semiclassical FT equation (6), as opposed to Eq. (9) that relates the electron density to the quantum-mechanical Green's function.

The self-consistent solution in quantum transport or electronic structure calculations is often found using a "simple mixing" method, where the charge density (or the total potential) on the $m+1$ iteration loop is updated through the input n_{in}^m and output n_{out}^m densities on the previous m iteration $n_{in}^{m+1}=(1-\epsilon)n_{in}^m+\epsilon n_{out}^m$, with ϵ being a small constant, $\sim 0.1-0.01$. Typically needed are $\sim 200-2000$ iteration steps to achieve our convergence criteron

$$\frac{|n_{out}^m - n_{in}^m|}{n_{out}^m + n_{in}^m} < 10^{-5}. \tag{12}$$

In order to improve the convergence, we employ the modified Broyden's second method,[38] which allows us to reduce drastically the number of iteration steps to $\sim 15-40$. An input charge density for $m+1$ iteration is constructed from the sets of input and output densities from all m previous iterations

$$n_{in}^{m+1} = n_{in}^m - B^1F^m - \sum_{j=2}^{m} U^j(V^j)^TF^m,$$

$$F^m = n_{out}^m - n_{in}^m,$$

$$U^i = -B^1(F^i - F^{i-1}) + n_{in}^i - n_{in}^{i-1} - \sum_{j=2}^{i-1} U^j(V^j)^T(F^i - F^{i-1}),$$

$$(V^i)^T = \frac{(F^i - F^{i-1})^T}{(F^i - F^{i-1})^T(F^i - F^{i-1})}. \tag{13}$$

The initial guess B^1 is taken to be a small constant so that the input to the second iteration is effectively constructed using the simple mixing ($B^1=\epsilon$). The scheme given by Eqs. (13) requires the storage of relatively small number vectors,

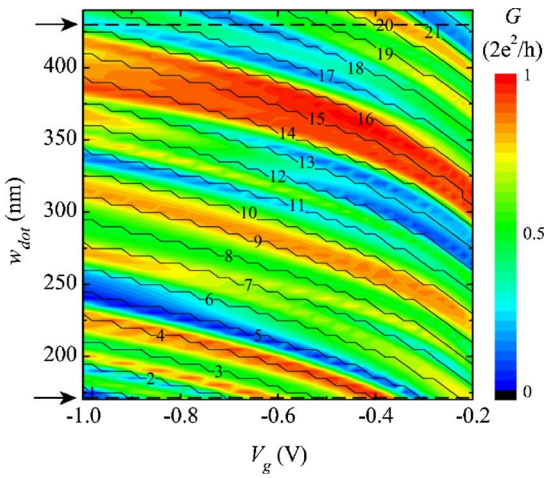

FIG. 3. (Color online) The conductance of the open quantum dot as a function of the width, w_{dot}, and the gate voltage V_g calculated within the Hartree approximation. Solid thin lines denote the number of electrons. (Note that a zigzag-type behavior of the electron number is an artifact due to finite grid steps.) Arrows indicate $w_{dot}=170$ nm and $w_{dot}=430$ nm corresponding to two regimes, $\Delta \gg \Gamma$ and $\Delta \sim \Gamma$, discussed in Sec. IV.

which is, thus, more effective than the original Broyden's second method.

IV. RESULTS AND DISCUSSION

A. Few-electron open dot

We calculate the magnetotransport of a split-gate open quantum with the following parameters representative of a typical experimental structure. The 2DEG is buried at $b=60$ nm below the surface (the widths of the cap, donor, and spacer layers are 10, 36, and 14 nm, respectively) and the donor concentration is 0.6×10^{24} m^{-3}. The width of the semi-infinitive leads is $w_{lead}=540$ nm and the width of the constrictions is $w_{qpc}=100$ nm (both quantum point contacts are identical), see Fig. 1(b). The length of the quantum dot is kept constant throughout the paper, $l_{dot}=160$ nm, while the width of the dot is varied in the range $w_{dot}=170-440$ nm. The gate voltages applied to the gates are $V_{lead}=-0.4$ V and $V_{qpc}=-0.44$ V. With these parameters of the device, there are 14 channels available for propagation in the leads, and the electron density in the center of the leads is $n_{lead}=1.6\times10^{15}$ m^{-2}. The maximal electron density in the dot (for $w_{dot}=440$ nm) is also $n_{dot}=1.6\times10^{15}$ m^{-2}. The temperature is fixed at $T=0.2$ K for all results presented below.

In the following, we discuss the open quantum dot with $N=1$ propagating channel through both quantum point contacts. Note that increasing the number of propagating channels to $N=2$ and 3 does not qualitatively change the results presented below. In order to set up the QPCs in the one-mode regime, we grounded one of them and studied the conductance of the remaining QPC as a function of the gate voltage V_{qpc}. The calculated conductance shows a characteristic steplike dependence and we choose V_{qpc} at the first conductance plateau, namely, $V_{qpc}=-0.44$ V.

Figure 3 shows the plot of the conductance G as a function of the dot width w_{dot} and the gate voltage V_g (the magnetic field is restricted to zero). The distinctive feature of the open quantum dots is the oscillations of the conductance in response to the change of the geometrical size or the Fermi energy. (Various aspects of the conductance oscillations in small and large dots have been the subject of numerous experimental and theoretical works during the past decade[1].) In the present study, we concentrate on two dots with $w_{dot}=170$ nm and $w_{dot}=430$ nm (as indicated by arrows in Fig. 3). As will be shown below, the first dot corresponds to the transport regime when $\Delta \gg \Gamma$ (single-level transport regime), whereas the second dot operates in the regime $\Delta \sim \Gamma$ (regime of overlapping resonances), where $\Delta=\frac{2\pi\hbar^2}{m^*S_a}$ is the mean level spacing separation in the dot with the actual area S_a, and Γ is the lead-induced broadening of the resonant energy levels. Note that in relatively large dots the condition $\Delta \gg \Gamma$ can be achieved only in the Coulomb blockade regime when the level broadening Γ is small because of the weak coupling to the leads. However, several groups have demonstrated theoretically and experimentally that for small few-electron quantum dot, the single-level transport $\Delta \gg \Gamma$ can be achieved even in the open dot transport regime, where the electron number in the dot is not quantized and the Coulomb charging is unimportant.[5,9,40]

It is worthy to note that a linear change of the gate voltage leads to a nonlinear change of the effective dot size. (If it were linear, the conductance oscillations in Fig. 3 would exhibit a perfect linear-stripe-type pattern.) This is consistent with the experimental results of Ref. 39 that show a deviation from the linear dependence of the gate depletion distance as the gate voltage was varied.

B. Regime $\Delta \gg \Gamma$: Single-level transport regime

Figure 4 shows the number of electrons in the few-electron open quantum dot, the conductance, and the peak–energy-level position as a function of the gate voltage V_g for a quantum dot with $w_{dot}=170$ nm calculated in the Hartree, DFT, and TF approximations. [The Hartree approximation corresponds to disregarding the exchange-correlation potential in Eq. (3), $V_{xc}=0$.] The peak positions of the resonant energy levels in the dot are extracted from the calculated DOS, as illustrated in Fig. 4(c) for the case when the gate voltage $V_g=-0.6$ V. The estimation of the mean level separation gives $\Delta \approx 0.6$ meV (for $V_g=-0.6$ V), which agrees quite well with the actual level separation shown in Figs. 4(c)–4(e). (Note that within the given interval of variation of V_g, the actual dot area changes and hence Δ varies as well.) An inspection of the DOS shows that the separation between the resonant levels are much larger than the level broadening, $\Delta \gg \Gamma$. (Γ is loosely defined as the width of the resonant peaks in the DOS at the half maximum.)

All three approximations give very similar electron number N in the dot as a function of the gate voltage V_g. N monotonically increases with increase of V_g, which reflects the fact that in the open regime the chemical potential is constant throughout the whole system such that the electrons freely enter and leave the dot. However, the conductance calculated in the Hartree and DFT approximations exhibits

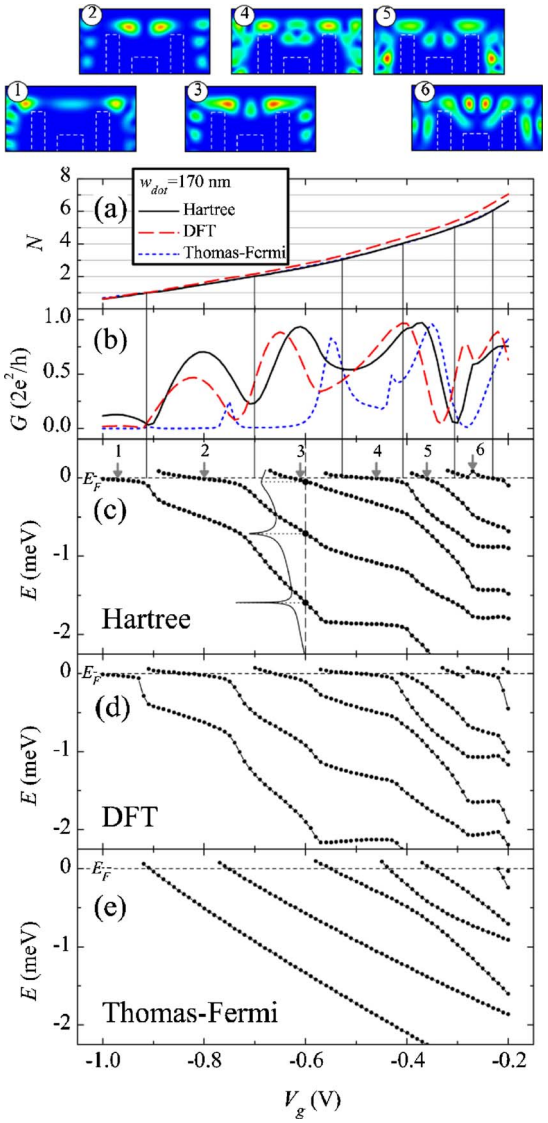

FIG. 4. (Color online) (a) The number of electrons, (b) the conductance, and (c)–(e) resonant energy structure in the few-electron open quantum dot with w_{dot}=170 nm calculated within the Hartree, DFT, and Thomas-Fermi approximations. The top panel shows the electron probability amplitudes $|\Psi(x,y)|^2$ for the resonant energy levels marked by arrows in (c). Inset in (c) shows the DOS for V_g =−0.6 V.

rather similar behavior, whereas the Thomas-Fermi conductance shows a very different gate voltage dependence. The origin of this difference can be understood from the analysis of the resonant level structure. The resonant energy levels calculated within the Hartree and DFT approximations *get pinned* to the Fermi energy, see Figs. 4(c) and 4(d), respectively. In stark contrast, the energy-level positions calculated in the Thomas-Fermi approximation sweep past the Fermi level in a linear fashion when the applied voltage is varied [Fig. 4(e)].

The effect of level pinning is related to the screening properties of the open quantum dot and the presence of the resonant structure in its DOS. Indeed, in the vicinity of the resonances, the DOS of the dot is enhanced such that electrons with the energies close to E_F (when $f_{FD}<1$) can easily screen the external potential. This leads to the metallic behavior of the system when the electron density in the dot can be easily redistributed to keep the potential constant. As a result, in the vicinity of a resonance, the system only weakly responds to the external perturbation (change of a gate voltage, magnetic field, etc.), i.e., the resonant levels become pinned to the Fermi energy. A comparison between the Hartree and DFT approximations indicates that the exchange-correlation interaction seems to enhance the pinning, but an overall change is small [cf. Figs. 4(c) and 4(d)]. Thus, in the following, we concentrate on the Hartree approximation only. In contrast to the Hartree and DFT approaches, the effect of pinning is absent in the TF approximation. This is because the total confining potential calculated within the TF approximation does not capture the resonant structure of the DOS. Note that a modeling of the magnetotransport in a quantum dot conceptually similar to our TF approach was performed by Bird *et al.*,[40] where the confining potential for every given gate voltage was obtained as a self-consistent solution of the Poisson equation. It is worth mentioning that the pinning of band edges at the Fermi energy is shown to occur in quantum wire, which is due to the $E^{-1/2}$ singularity in the density of states of electrons in one dimension.[41]

Conductance oscillations in the open quantum dots can be related to the presence and/or absence of the resonant energy levels at E_F. Indeed, the first three peaks in the Hartree conductance are attributed to the presence of corresponding resonant levels, which is confirmed by the inspection of the wave function $|\Psi(x,y)|^2$ (by counting the number of nodes of $|\Psi(x,y)|^2$) (Fig. 4). In turn, the dips indicate the absence of levels at E_F and agree precisely with integer N reflecting the fact that all the available levels are below E_F and thus are fully filled. Note that for less negative gate voltages ($|V| \lesssim 0.3$ V), the separation between the levels Δ becomes comparable to the broadening Γ, such that the dips in the conductance no longer correspond to the integer electron number N (see next section for details). It is also interesting to note that the resonant state corresponding to the fifth eigenstate (five nodes of the $|\Psi(x,y)|^2$) is situated lower in energy than the corresponding resonant state related to the fourth eigenstate. This is an indication that fifth state couples with the leads more strongly than fourth state.[42]

The pinning of the resonant energy levels has an important effect on transport in open quantum dots. In the considered transport regime, $\Delta \gg \Gamma$, the conductance calculated within the one-electron (TF) approximation exhibits distinct peaks separated by broad valleys of essentially zero conductance. This reflects the structure of the one-electron DOS, where the resonant levels sweep past the Fermi level in a linear fashion. In contrast, as a result of pinning, the DFT and Hartree conductances show much broader oscillations in comparison with the one-electron approach [Fig. 4(b)].

C. Regime $\Delta \sim \Gamma$: Regime of overlapping resonances

When an effective size of a quantum dot increases, the mean level spacing separation Δ decreases. For the quantum dot of the size w_{dot}=430, the estimation of the mean level

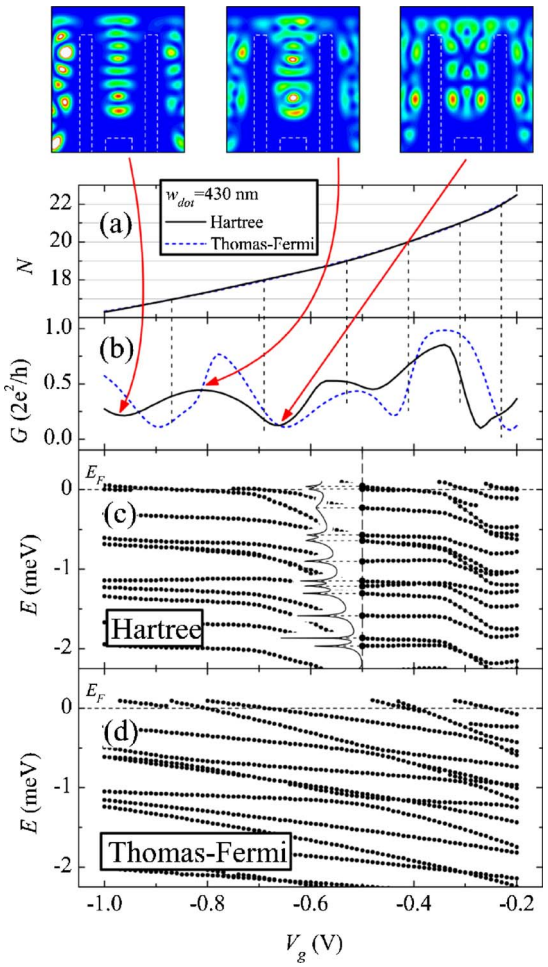

FIG. 5. (Color online) (a) The number of electrons, (b) the conductance, and (c) and (d) resonant energy structure in the few-electron open quantum dot with w_{dot}=430 nm calculated within the Hartree and Thomas-Fermi approximations. The electron probability amplitudes $|\Psi(x,y)|^2$ are shown for some representative V_g (top panel). Inset in (c) shows the DOS for V_g=−0.5 V.

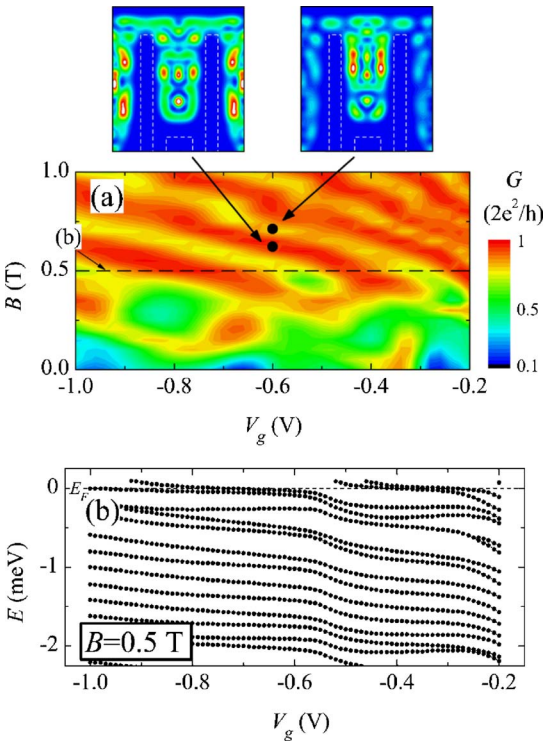

FIG. 6. (Color online) (a) The conductance of the open quantum dot as a function of the magnetic field B and gate voltage V_g for the open quantum dot of the width w_{dot}=430 nm calculated within the Hartree approximation. (b) The energy structure for B=0.5 T calculated within the Hartree approximation. The top panel shows the electron probability amplitudes $|\Psi(x,y)|^2$ (top) for two representative magnetic fields.

separation gives $\Delta \approx 0.15$ meV (for V_g=−0.6 V), which agrees quite well with the actual level separation shown in Figs. 5(c) and 5(d). An inspection of the DOS shows that for this dot the spacing between neighboring levels is comparable with the level broadening, $\Delta \sim \Gamma$, see Fig. 5(c). (Note that the level broadening is controlled by coupling to the leads and does not depend on the dot size.) Because neighboring levels start to overlap, there is always one or several energy states at E_F mediating transport through the dot. The effect of the pinning of the energy levels in the Hartree calculations (as well as its absence in the TF calculations) is also clearly seen in this regime. However, in contrast to the regime $\Delta \gg \Gamma$, the dips in the conductance can no longer be related to the integer number of electrons in the dot. Instead, it is the interference between states at the entrance and exit of the open quantum that determines the dependence $G=G(V_g)$.[42] Our preliminary results for the conductance of even larger dots (containing hundreds of electrons) outline different features of the TF and Hartree conductances that manifest themselves in the amplitude and the broadening of the conductance peaks. A detailed analysis of the statistics of the conductance oscillations is, however, outside the scope of the present work and will be deferred to future publications.

D. Effect of magnetic field

In a sufficiently high magnetic field, the electron transport takes place by the edge states with a characteristic dimension of the order of the magnetic length $l_B=\sqrt{\hbar/eB}$. In the edge state transport regime, backscattering on the potential defining the quantum dot decreases and, for a large enough B, electrons pass through the device with the transmission close to unity. Transport in such a regime is referred to as adiabatic. For the open quantum dot of w_{dot}=430 nm, transition to adiabatic propagation takes place at about $B \approx 0.5$ T, see Fig. 6(a). The conductance for $B \gtrsim 0.5$ T shows pronounced oscillations due to the Aharonov-Bohm interference. When the magnetic field changes such that the total magnetic flux $\Phi=BS$ through the dot is modified by the one flux quantum $\phi_0=h/e$, the conductance demonstrates periodic oscillations with the period $\Delta B=\phi_0/S$ (S is the characteristic area of the dot). Using the actual dot area S_a, we get ΔB=0.11 T, which is nearly twice less than extracted from Fig. 6(a), where ΔB=0.25 T. The discrepancy can be related to a finite extent of the edge state circulating inside the dot ($l_B \approx 35$ nm for B=0.5). As a result, the area enclosed by the edge state is

much smaller than the geometrical area of the dot.

The resonant energy structure is modified substantially when a magnetic field is applied, cf. Fig. 6(b) for $B=0.5$ T and Fig. 5(c) for $B=0$ T. The resonant levels exhibit almost equal separation, which can be related to the well-known Darvin-Fock-type energy spectrum formation for the corresponding closed dot.[43] The distinguished feature of the energy-level structure is much stronger pinning of the resonant levels to E_F that persists over larger intervals of V_g in comparison to the $B=0$ case. Stronger pinning can be attributed to the enhanced screening efficiency because of the increased localization of the wave function for the case of nonzero magnetic field. As we mentioned in the Introduction, the strong pinning of the resonant energy levels in the presence of the magnetic field can have a profound effect on transport properties of various devices operating in the edge state transport regime including the Mach-Zender[17] and Laughlin[18] interferometers as well as antidot devices.[19–22]

To conclude this section, it is worth mentioning that another manifestation of the pinning in the edge state regime is the well-known effect of the formation of the compressible and incompressible strips near the structure boundary.[10]

E. Open versus closed system

In modeling quantum-mechanical transport in quantum dots and related systems, one often uses an approximation where an inherently open system is replaced by a corresponding large but closed one, see, e.g., Ref. 44. In this section, we critically examine such an approximation. In particular, we address the question whether a conductance calculated in such a way coincides with the conductance of a truly open system and whether the pinning of the resonant energy levels survives or not. For modeling of the closed system, we replace the semi-infinitive leads by the potential walls of an infinitive height such that the solution of the Schrödinger equation reduces to the eigenproblem

$$H\psi = E\psi, \tag{14}$$

where E and ψ are discrete sets of eigenvalues and eigenvectors, and the Hamiltonian H is given by Eq. (1). We solve Eq. (14) self-consistently by performing the fast Fourier transformation from the coordinate into the energy space, which greatly reduces computational cost.

In our calculations, we fix the Fermi energy such that the charge density in the system is given as

$$n(\mathbf{r}) = \sum_i \psi_i(\mathbf{r}) f_{FD}(E_i - E_F). \tag{15}$$

This assumption leads to a noninteger electron number in a system, but we a priori construct the closed system resembling the open one as much as possible. Note also that because the total number of electrons $N_{tot} \gg 1$, the effect of the noninteger N_{tot} on the total potential is practically negligible.

In order to calculate the conductance of the system at hand, we cut off slices in the vicinity of the boundaries as illustrated in Fig. 7(a) and then add homogeneous semi-infinite leads with the potential that matches the potential of the boundary slices. Finally, we solve a scattering problem for this given potential using the recursive Greens's-function technique.[12]

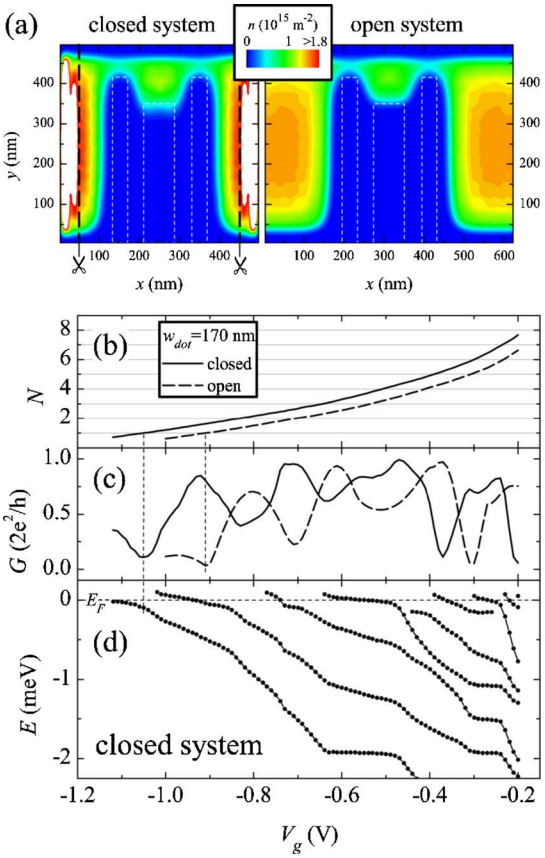

FIG. 7. (Color online) (a) The representative self-consistent charge densities for the closed and open systems. The thick dashed lines show the cuts for the transport calculations. (b) The electron number, (c) the conductance, and (d) the energy structure calculated within the Hartree approximation in the closed-system approximation. The dashed lines denote the result for the open system (the same as in Fig. 4). The width of the quantum dot is $w_{dot}=170$ nm.

Figures 7(b)–7(d) show the electron number in the dot N, the conductance G, and the resonant energy structure within the Hartree approximation. The comparison to the corresponding results for the open system shows that the closed-system approximation reproduces all the results not only qualitatively but rather quantitatively, cf. Fig. 4. The only difference is the shift along V_g axis, which is simply related to the fact that the Hartree potential for the case of the closed system, in contrast to the open one, does not include a contribution from the semi-infinite leads. Figure 7(d) reveals that the pinning of resonant energy levels to the Fermi energy is present in the closed-system approximation as well. We thus conclude that this approximation might be used for the modeling of the transport properties and the resonant energy-level structure of the corresponding open system. We, however, should note that with the present approximation we could not satisfy the convergence criterion (12) that we routinely use for the calculation of the conductance in the open systems as described in Sec. III.

V. CONCLUSION

We have developed an approach for full quantum-mechanical many-body magnetotransport calculations in open systems that starts from the lithographical layout of the device and does not include phenomenological parameters such as coupling strengths, charging constants etc. The whole device, including semi-infinitive leads, is treated in the same footing (i.e., the electron-electron interaction is accounted for in both the leads as well as in the dot region). The many-body effects are included within the DFT and Hartree approximations. The developed approach is valid in the open transport regime when the conductance of each QPC connecting the dot to the reservoir exceeds (or equal) the conductance unit $G_0=2e^2/h$, such that the electron number in the dot is not quantized and the Coulomb charging is unimportant.

The developed method was applied to calculate the conductance through an open quantum dot. The main finding of the present paper is the effect of pinning of the resonant levels to the Fermi energy due to the enhanced screening. Our results represent a significant departure from a conventional picture where a variation of external parameters (such as a gate voltage, magnetic field, etc.) causes the successive dot states to sweep past the Fermi level in a linear fashion. We instead demonstrate the highly nonlinear behavior of the resonant levels in the vicinity of the Fermi energy. We show that the pinning effect is absent in a one-electron (Thomas-Fermi) approximation because, in this case, the self-consistent potential does not account for the resonant structure of the DOS in the dot. The pinning of the resonant levels in open quantum dots leads to the broadening of the conduction oscillations in comparison to the one-electron picture. It remains to be seen whether accounting for this effect might shed new light on the interpretation of the conductance oscillation statistics in open quantum dots.

The pinning of the resonant levels becomes much more pronounced in the presence of the perpendicular magnetic field. This can be attributed to the enhanced screening efficiency because of the increased localization of the wave function. The strong pinning of the resonant energy levels in the presence of magnetic field can have a profound effect on transport properties of various devices operating in the edge state transport regime including Mach-Zender[17] and Laughlin[18] interferometers as well as antidot devices.[19–22]

We should stress that the pinning effect predicted in this paper is not specific to the considered material system (GaAs/AlGaAs heterostructure) and is expected to hold in any two-dimensional system in open transport regime (e.g., Si inversion layer structures, etc.).

Finally, in the present paper, we critically examined an approximation used in modeling the quantum-mechanical transport in quantum dots and related systems when an inherently open system is replaced by a corresponding large but closed one.

In the present study, we have limited ourselves to the case of spinless electrons. Work is in progress to include the effect of the spin in order to revisit the effect of spin splitting recently observed in open quantum dots.[9,37]

ACKNOWLEDGMENTS

S.I. acknowledges financial support from the Swedish Institute and the EU network SINANO. Numerical calculations were performed in part using the facilities of the National Supercomputer Center, Linköping, Sweden.

[1] For a review, see, e.g., C. W. J. Beenakker, Rev. Mod. Phys. **69**, 731 (1997); Y. Alhassid, *ibid.* **72**, 895 (2000).
[2] S. Datta, Nanotechnology **15**, S433 (2004).
[3] For a review, see, e.g., M. Kastner, Ann. Phys. **9**, 885 (2000).
[4] M. Ciorga, A. S. Sachrajda, P. Hawrylak, C. Gould, P. Zawadzki, S. Jullian, Y. Feng, and Z. Wasilewski, Phys. Rev. B **61**, R16315 (2000).
[5] I. V. Zozoulenko, A. S. Sachrajda, C. Gould, K.-F. Berggren, P. Zawadzki, Y. Feng, and Z. Wasilewski, Phys. Rev. Lett. **83**, 1838 (1999).
[6] T. K. Ng and P. A. Lee, Phys. Rev. Lett. **61**, 1768 (1988); L. I. Glazman and M. E. Raikh, JETP Lett. **47**, 452 (1988).
[7] L. E. Henrickson, A. J. Glick, G. W. Bryant, and D. F. Barbe, Phys. Rev. B **50**, 4482 (1994).
[8] K. M. Indlekofer, J. P. Bird, R. Akis, D. K. Ferry, and S. M. Goodnick, J. Phys.: Condens. Matter **15**, 147 (2003).
[9] M. Evaldsson, I. V. Zozoulenko, M. Ciorga, P. Zawadzki, and A. S. Sachrajda, Europhys. Lett. **68**, 261 (2004).
[10] D. B. Chklovskii, B. I. Shklovskii, and L. I. Glazman, Phys. Rev. B **46**, 4026 (1992).
[11] For a review, see, e.g., S. M. Reimann and M. Manninen, Rev. Mod. Phys. **74**, 1283 (2002).
[12] I. V. Zozoulenko, F. A. Maaø, and E. H. Hauge, Phys. Rev. B **53**, 7975 (1996); **53**, 7987 (1996); **56**, 4710 (1997).
[13] B. Tanatar and D. M. Ceperley, Phys. Rev. B **39**, 5005 (1989).
[14] G. F. Giuliani and G. Vignale, *Quantum Theory of the Electron Liquid* (Cambridge University Press, Cambridge, 2005).
[15] See, e.g., H. Saarikoski, E. Räsänen, S. Siljamäki, A. Harju, M. J. Puska, and R. M. Nieminen, Phys. Rev. B **67**, 205327 (2003).
[16] I. P. Radu, J. B. Miller, S. Amasha, E. Levenson-Falk, D. M. Zumbuhl, M. A. Kastner, C. M. Marcus, L. N. Pfeiffer, and K. W. West (unpublished); S. Ihnatsenka and I. V. Zozoulenko (unpublished).
[17] Y. Ji, Y. Chung, D. Sprinzak, M. Heiblum, D. Mahalu, and H. Shtrikman, Nature (London) **422**, 415 (2003).
[18] F. E. Camino, W. Zhou, and V. J. Goldman, Phys. Rev. B **72**, 075342 (2005).
[19] See, e.g., S. Das Sarma, M. Freedman, and C. Nayak, Phys. Today **59**(7), 32 (2006), and references therein.
[20] C. J. B. Ford, P. J. Simpson, I. Zailer, D. R. Mace, M. Yosefin, M. Pepper, D. A. Ritchie, J. E. F. Frost, M. P. Grimshaw, and G. A. C. Jones, Phys. Rev. B **49**, 17456 (1994); M. Kataoka, C. J. B. Ford, G. Faini, D. Mailly, M. Y. Simmons, and D. A. Ritchie, *ibid.* **62**, R4817 (2000).
[21] I. Karakurt, V. J. Goldman, J. Liu, and A. Zaslavsky, Phys. Rev. Lett. **87**, 146801 (2001); M. Kataoka and C. J. B. Ford, *ibid.* **92**,

199703 (2004); V. J. Goldman, *ibid.* **92**, 199704 (2004); S. Ihnatsenka and I. V. Zozoulenko, Phys. Rev. B **74**, 201303(R) (2006).
[22] I. V. Zozoulenko and M. Evaldsson, Appl. Phys. Lett. **85**, 3136 (2004).
[23] N. D. Lang, Phys. Rev. B **52**, 5335 (1995).
[24] J. Taylor, H. Guo, and J. Wang, Phys. Rev. B **63**, 245407 (2001).
[25] P. S. Damle, A. W. Ghosh, and S. Datta, Phys. Rev. B **64**, 201403(R) (2001).
[26] F. Evers, F. Weigend, and M. Koentopp, Phys. Rev. B **69**, 235411 (2004).
[27] C. Toher, A. Filippetti, S. Sanvito, and K. Burke, Phys. Rev. Lett. **95**, 146402 (2005).
[28] M. Koentopp, K. Burke, and F. Evers, Phys. Rev. B **73**, 121403(R) (2006).
[29] J. J. Palacios, Phys. Rev. B **72**, 125424 (2005).
[30] S.-H. Ke, H. U. Baranger, and W. Yang, arXiv:cond-mat/0609637 (unpublished).
[31] S. Ihnatsenka and I. V. Zozoulenko, arXiv:cond-mat/0703380, Phys. Rev. B (to be published); arXiv:cond-mat/0701657 (unpublished).
[32] J. H. Davies, I. A. Larkin, and E. V. Sukhorukov, J. Appl. Phys. **77**, 4504 (1995).
[33] J. Martorell, H. Wu, and D. W. L. Sprung, Phys. Rev. B **50**, 17298 (1994).
[34] S. Datta, *Electronic Transport in Mesoscopic Systems* (Cambridge University Press, Cambridge, 1997).
[35] S. Ihnatsenka and I. V. Zozoulenko, Phys. Rev. B **73**, 075331 (2006); **73**, 155314 (2006).
[36] Y. Wang, J. Wang, H. Guo, and E. Zaremba, Phys. Rev. B **52**, 2738 (1995).
[37] M. Evaldsson and I. V. Zozoulenko, Phys. Rev. B **73**, 035319 (2006).
[38] D. Singh, H. Krakauer, and C. S. Wang, Phys. Rev. B **34**, 8391 (1986).
[39] I. V. Zozoulenko, A. S. Sachrajda, P. Zawadzki, K.-F. Berggren, Y. Feng, and Z. Wasilewski, Phys. Rev. B **58**, 10 597 (1998).
[40] J. P. Bird, R. Akis, and D. K. Ferry, Phys. Rev. B **60**, 13676 (1999).
[41] K. Hirose, S.-S. Li, and N. S. Wingreen, Phys. Rev. B **63**, 033315 (2001).
[42] I. V. Zozoulenko and K.-F. Berggren, Phys. Rev. B **56**, 6931 (1997).
[43] J. Davies, *The Physics of Low-Dimensional Semiconductors* (Cambridge University Press, Cambridge, 1998).
[44] D. Jovanovic and J.-P. Leburton, Phys. Rev. B **49**, 7474 (1994); K.-F. Berggren and I. I. Yakimenko, *ibid.* **66**, 085323 (2002).